

# An Aerodynamic Study of Multirotor Uncrewed Aircraft System Using Motion Capture Technology

Rachael Lander\* and Megan Wolfe†  
Mississippi State University, Mississippi State, MS, 39762

Motion capture technology is a method of data acquisition that provides precise position and orientation data for a rigid body. This technology has been utilized to study the aerodynamic and stability properties of fixed wing Uncrewed Aircraft Systems (UAS), but there is less documented research on multirotor aircraft. The purpose of this paper is to establish the reliability of data that can be acquired and analyzed using this method on a multirotor UAS. The Hawk's Work F450 Drone Kit A was selected as the test subject due to its open-source autopilot system, Pixhawk, which allows the user to customize a variety of parameters. The kit was assembled using the manual provided and instructional videos found online. Once the UAS was built, features such as the compass, radio, and Electronic Speed Controllers (ESC) were calibrated. After undergoing flight testing to learn how the UAS and the motion capture technology system perform, three flight patterns were selected, hover, straight and level, and a square maneuver, which allowed the six degrees of freedom to be tested. The OptiTrack System, consisting of twelve Primex41 cameras, recorded the time and position of four probes arranged in a triangular configuration on the UAS. Additional flight parameters, such as altitude, power, and thrust, were gathered from the onboard Pixhawk autopilot. To process the data in MATLAB, it was first transformed from the earth frame to the body frame using rotation matrices, then filtered with a Savitzky-Golay function to reduce noise in the dataset. After, derivatives can be computed from positional data to find the velocity and acceleration. These along with their rotational counterparts can then be plotted against time for each maneuver to view the aerodynamic and stability properties of the UAS.

## I. Nomenclature

$\dot{V}_b$	=	Acceleration in Body Axis
$\omega$	=	Angular Acceleration
$cm$	=	Centimeters
$b$	=	Body-Referenced Axis System
$R^2$	=	Coefficient of Determination
$C$	=	Cosine
$deg$	=	Degrees
$D$	=	Drag
$A$	=	Drag Force Coefficient
$e$	=	Earth-Referenced Axis System
$ESC$	=	Electronic Speed Controller
$GPS$	=	Global Positioning System
$g$	=	Gravity
$Hz$	=	Hertz
$I$	=	Inertia
$m$	=	mass
$MOCAP$	=	Motion Capture System
$\vec{r}$	=	Offset Vector
$\theta$	=	Pitch

---

\*Undergraduate Senior, ASE Department, AIAA Student Member

†Undergraduate Senior, ASE Department, AIAA Student Member

$q$	=	Pitch rate
$x$	=	Position on the x axis
$y$	=	Position on the y axis
$z$	=	Position on the z axis
$\phi$	=	Roll
$p$	=	Roll rate
$R$	=	Rotation Matrix
$RPM$	=	Rotations Per Minute
$S$	=	Sine
$\sigma$	=	Standard Deviation
$T$	=	Thrust
$\tau$	=	Torque
$UAS$	=	Uncrewed Aircraft System
$\dot{x}$	=	Velocity on the x axis
$\dot{y}$	=	Velocity on the y axis
$\dot{z}$	=	Velocity on the z axis
$\psi$	=	Yaw
$r$	=	Yaw rate
$V_b$	=	Velocity in Body Axis

## II. Introduction

THE aerodynamics of a Multirotor Uncrewed Aircraft Systems (UAS) when flying in translational and hover flight can be evaluated using a variety of methods. Some examples of these are wind tunnel testing, computational fluid dynamics, and motion capture technology (MOCAP)[1]. The Autonomous Systems Research Laboratory, located at Mississippi State University's Raspet Flight Laboratory, houses an OptiTrack System with twelve Primex41 cameras. This system has been used in past experiments by the university, but only for fixed wing aircraft. This made the motion capture methodology the most cost-effective option due to the availability of resources and subject matter experts within the Aerospace Engineering Department. The cameras track and collect time, location, and attitude data by recognizing probes that are attached to the test subject, creating a rigid body. The data can be processed to gain a variety of outputs depending on the goal of research.

The dynamics of a quadcopter rely on the rotors and propellers which generate thrust. In takeoff, the rotors will be spinning at a speed such that the thrust is greater than the weight, but in hover, the thrust must equal the weight to remain stationary. By adjusting the speed of each individual rotor, the thrust distribution can be changed which allows the user to control the motion allowing lateral movement. Opposing rotor pairs spin in opposite directions to cancel out reactive torque, but if the rotor speeds are unbalanced, the body will rotate. Quadcopters have six degrees of freedom, three translational (x, y, z) and three rotational (pitch, roll, and yaw). By modeling and extrapolating from these, the equations of motion can be determined and plotted.

The type of UAS selected was a quadcopter which is a multirotor aircraft with four rotors as the name suggests. The Hawk's Work F450 Drone Kit A[2] is a comprehensive UAS kit that is marketed to beginner and advanced UAS hobbyists due to its pre-soldered connections and customizability. It comes with all the parts needed for assembly and control including a Pixhawk autopilot system and a Flysky remote, and more components can be added or exchanged to enhance the capabilities of the UAS. The Pixhawk autopilot is an open-source flight management system used on the quadcopter. It is compatible with Mission Planner[3] which is a software used to control flight modes and parameters, download data, and program flights. The Flysky remote is used for manual flight and communicates with the receiver onboard the UAS.

The purpose of this paper is to determine the feasibility of accurately creating and plotting the six degrees of freedom of a quadcopter using the position and time data captured using MOCAP. The velocities and accelerations were derived, and the data will be used comprehensively to determine thrust and drag. The motion capture data will be supplemented with data acquired from the autopilot system to account for aliasing, which is the misidentification of frequency, caused by the high rotational speed of the rotors compared to the frame capture speed.

### III. Methods

To test the aerodynamic characteristics of a multirotor UAS, a basic understanding of multirotor flight and stability is needed. Another key factor is having the testing equipment required and a safe testing environment to achieve the best data possible.

#### A. Research

The research began by talking with various professors about what capabilities Mississippi State University had regarding UAS testing along with aerodynamics research. Previous research had been conducted by Mohamed El Mehdi Oubahi, Shreyas Narsipur, and Jichul Kim using MOCAP to capture aerodynamic data on various fixed wing UAS vehicles. This research project expands the research previously conducted and adds the new challenge of using a multirotor UAS. Previous research from Oubahi also included a validation of the motion capture system by accurately tracking and comparing the vertical acceleration reported by MOCAP to the local acceleration due to gravity[4].

Preliminary research began by gaining a better understanding of the aerodynamics of a multirotor UAS along with the stability equations. Various articles were reviewed on similar experimentation on fixed wing aircraft, multirotor flight, and other ways of capturing similar data. The UAS multirotor provided many challenges such as the rotations per minute (RPM) which needed to be captured due to aliasing being present because of the camera's shutter speed. When deciding which aircraft was best suited for testing, an open-source auto pilot was critical to be able to control the parameters measured, such as RPM.

#### B. Aircraft Assembly

The aircraft used in testing is the Hawk's Work F450 Drone Kit A shown in (Fig 1). Assembly was performed following provided instructions in the kit along with online video tutorials[5]. The process began with building the frame by attaching the four arms of the UAS to the middle section's top and bottom piece. The two red arms are the forward portion of the aircraft while the two white arms are the aft. Second, the brushless motors were connected to each arm paying close attention to which direction the motor was labeled to rotate to ensure similar motors were diagonal from one another. Third, the vibration dampening plate was fixed to the middle section of the frame using adhesive strips. Fourth, The Pixhawk autopilot was attached on top of the vibration dampening plate using adhesive strips. Fifth, the four electronic speed controllers (ESC) were attached to each motor and into the respective port on the autopilot. Sixth, additional systems located within the kit such as the global positioning system (GPS) module, safety switch, buzzer, power module, and receiver were connected to the autopilot. Seventh, the receiver was connected to the remote controller using the binding tool to receive signal and modifying various settings within the flight controller. Eighth, once the battery was fully charged a Velcro strip was added to ensure the battery stayed fixed during flight. Ninth, after Mission Planner was downloaded onto a computer, calibration began for the compass, radio, flight modes, fail safe, and ESCs. Finally, the aircraft was ready for flight.



**Fig. 1 Hawk's Work F450 Drone Kit Prior to Assembly.**



**Fig. 2 Hawk's Work F450 Drone Assembled.**

During the aircraft assembly process, troubleshooting was needed. The instructions provided with the kit were vague and the assemblers were novice UAS builders. The first problem encountered was the ESCs would not rotate during the calibration stage which was resolved by flipping the positive and negative end of each ESC cable into the autopilot.

Switching the cables also turned on all audible tones the autopilot and buzzer provided to indicate various set up steps. Along with the audible tones, the autopilot also indicates visually the status using various colors and flashing or solid lights which became helpful in troubleshooting. The colors were researched online to have a better understanding of the status. After all motors could rotate, a violent oscillation was present when the aircraft was armed, and the aircraft would not take off. It was discovered that one of the motors was spinning in the wrong direction along with the autopilot having a bad port which caused one motor to rotate slower. This was remedied by flipping the two outer ESC connections into the motor and reprogramming the fifth port to support the autopilot-motor connection. The completed aircraft is shown in (Fig 2). The aircraft was then ready for the first flight which occurred on November 20th, 2024.

### C. Motion Capture Technology

The Autonomous Systems Research Laboratory has previously conducted similar research using fixed wing UAS[6]. This research helped guide the authors on what to expect and the capabilities of the laboratory. Due to the frequency of the motors being higher than what the cameras could capture, aliasing was present. To eliminate this, it was critical that RPM be calculated or measured.

The Motion Capture Laboratory is located at Mississippi State University's Raspet Flight Laboratory within the Autonomous Systems Research Laboratory shown in (Fig 3). The testing environment uses an OptiTrack system with twelve Primex41 cameras and the Motive computer software[7]. Prior to testing, calibration is required by using a wand and slowly moving throughout the testing area. Prior to all testing a calibration was performed at the origin point of the x, y, and z directions are set by placing a device at this point shown in (Fig 4). Five probes were attached to the UAS in triangulation, the cameras were then activated to recognize these probes and assign them as a rigid body. The MOCAP system captures data a frequency of 200 Hz.



**Fig. 3 The Autonomous Systems Research Laboratory.**

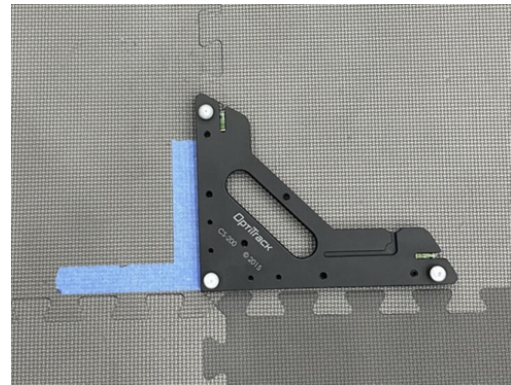


**Fig. 4 Calibration Device for the Origin of Testing Environment.**

### D. Data Acquisition

Testing and experimentation were performed using the OptiTrack system in the Autonomous Systems Research Laboratory. Three flight paths selected to be used in the experimentation: hover, straight and level, and a square motion. Each flight path was performed three times and recorded by OptiTrack cameras. The data for each flight were then downloaded for processing in MATLAB[8]. The data on board was downloaded from the Pixhawk system using Mission Planner.

During the early testing phase of the F450 Hawkworks UAS, a stability issue was found when the landing gear was installed, which caused it to shake violently and struggle to lift off. The landing gear was removed for the data collection process. Additionally, the use of the flight controller trim was modified to prevent the aircraft from rotating due to the ground effect during take-off and assist the pilot while flying the various flight paths.

All testing was completed in an indoor testing environment, which caused the GPS to not be able to pick up the signal. This limited the testing to manual piloted flight only, which led to some inconsistencies in positioning because the UAS pilot was a beginner. This will be taken into account by taking multiple sets of data for each flight path.



**Fig. 5 TSRC Q7 UAS.**

Due to persistent stability issues, the TSRC Q7 was chosen for the results provided. This quadcopter is shown below in (Fig 5).

### E. Methodology

The Optitrack system creates a rigid frame by triangulating the earth-referenced position of markers placed on the aircraft and returns the positional  $([x_e \ y_e \ z_e])$  and Euler angles  $(\phi \ \theta \ \psi)$  data in the earth-referenced axis system. An offset vector was applied to shift the generated center of geometry to the center of gravity of the quadcopter ( $||\vec{r}|| = [0.02, 0, -0.025]$ ). The third order linear regression filter implementing the Savitzky-Golay algorithm was used for position and attitude smoothing. Upon analyzing the  $R^2$  values for each flight, all filters yielded values above 0.985 for all measured variables.

The matrix ( $R$ ) is applied to transform the earth-referenced frame to the body-referenced frame is given by,

$$R = \begin{bmatrix} \cos(\theta)\cos(\psi) & \cos(\theta)\sin(\psi) & -\sin(\theta) \\ -\cos(\phi)\sin(\psi) + \sin(\phi)\sin(\theta)\cos(\psi) & \cos(\phi)\cos(\psi) + \sin(\phi)\sin(\theta)\sin(\psi) & \sin(\phi)\cos(\theta) \\ \sin(\phi)\sin(\psi) + \cos(\phi)\sin(\theta)\cos(\psi) & -\sin(\phi)\cos(\psi) + \cos(\phi)\sin(\theta)\sin(\psi) & \cos(\phi)\cos(\theta) \end{bmatrix} \quad (1)$$

and the angular acceleration  $\omega$ , whose components  $(p, q, r)$  are calculated as,

$$\begin{bmatrix} p \\ q \\ r \end{bmatrix} = \begin{bmatrix} 1 & 0 & -\sin(\theta) \\ 0 & \cos(\phi) & \sin(\phi)\cos(\theta) \\ 0 & -\sin(\phi) & \cos(\phi)\cos(\theta) \end{bmatrix} \begin{bmatrix} \dot{\phi} \\ \dot{\theta} \\ \dot{\psi} \end{bmatrix} \quad (2)$$

In the body frame, the force required for the acceleration of mass ( $m\dot{V}_b$ ) and the centrifugal force ( $\omega^T \times mV_b$ ) are equal to the gravity and thrust of the rotors,

$$m\dot{V}_b + \omega^T \times mV_b = R^T G + T_b \quad (3)$$

Additionally, the external torque in the body frame is given by,

$$\tau = I\dot{\omega} + \omega \times (I\omega) \quad (4)$$

Detailed equations were present in previous work conducted by Ouhabi et al. [6, 9, 10]

Using the method outlined by Sanca [11], the inertial matrix was calculated using geometric features of the aircraft and mass of the main body and motors.

The key parameters used from the UAS's ECS's were time, voltage, and current which all came from data captured from the battery. The voltage and current were used to compute power. This power demonstrated the total power from the battery used to power UAS including the four motors. Air density, area of the four rotors, and the power from the battery were used to compute thrust at each data point. Thrust could then be plotted against time to confirm that in hover, thrust equals weight. This thrust data was also used to create the thrust matrix,  $T_B$ .

## IV. Results and Discussion

The initial objective of this project was to validate the motion capture system by comparing experimental results. However, after further research, the team determined that a more effective approach would be to assess whether the data extracted from experimentation could be represented through stability equations and graphical analysis. Given the novelty of using a quad-copter for this type of study, the results obtained will provide insights into the feasibility of motion capture as a tool for quad-copter analysis.

The following subsections present flight results from three case studies: hover flight, forward straight-level flight, and the square flight path maneuver.

### A. Hover

Due to the difficulty in maintaining hover with the F450 Hawk, the TSRC Q7 was selected for testing. The flight test was divided into three phases: takeoff, hover, and landing. For this analysis, only data from the hover phase is presented in (Fig. 6).

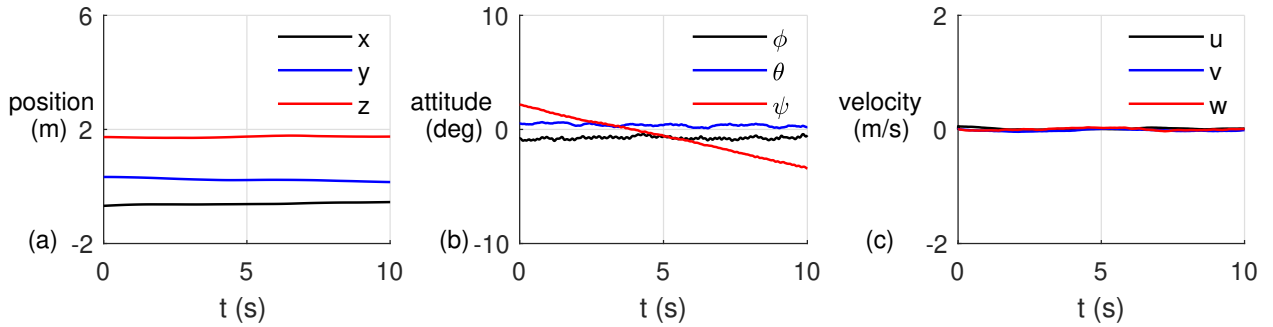


**Fig. 6 Hover flight data for the TSRC Q7: (a) Position time history, (b) attitude time history, and (c) velocity time history.**

During the hover phase, the quadcopter maintained an altitude of (1.7 m) with minimal variation, (Fig. 6(a)). Additionally, movement in the  $x$  and  $y$  directions remained minimal. The attitude data is depicted in (Fig. 6(b)), showing that pitch and roll were maintained, while minimal yaw drift ( $\pm 3^\circ$ ) was observed, likely due to external factors. In hover, the velocity in all axes is zero, as shown in (Fig. 6(c)). Therefore, (eqn. 3) simplifies to  $(T_b = \frac{mg + D_z}{R_{3,3}})$ , where only the thrust force in the  $z$ -direction acts to counterbalance the weight of the quad-copter. The drag in  $z$ -direction is assumed to be zero because ( $w = 0$ ), and ( $R_{3,3}$ ) is the third row, third column element of the rotation matrix.

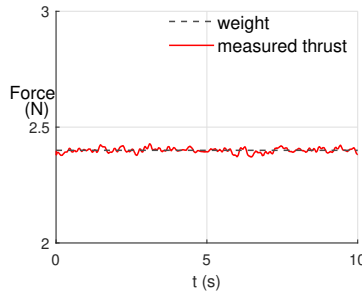


**Fig. 7 Measured thrust for the TSRC Q7 compared to its weight during hover.**

The measured thrust is plotted and compared to the weight of the TSRC Q7, as shown in (Fig. 7). The results are consistent with the expected trends, with minimal deviation observed. The maximum residual observed is ( $\pm 0.0285$  N) when comparing the measured thrust to the theoretical hover thrust.

### B. Forward Level Flight

Straight forward level flight was performed after the drone settled. The command input generated a tilt angle, while the thrust was maintained constant near the hover state which allowed for the altitude to be maintained at (1.5 m),



the forward flight maneuver was performed over (6 m) in the x-direction as shown in (Fig. 6(a)). Additionally, the attitude was maintained constant, with only the pitch angle being perturbed to achieve the desired flight path. The maneuver resulted in the velocity components in the y and z directions tending to zero, with a near-constant velocity in the x-direction ( $u \approx 1\text{ m/s}$ ) as depicted in (Fig. 6(c)).

The drag force along the coordinate axes, which is directly proportional to the velocity components in the corresponding directions ( $F_D = [A_x \dot{x}, A_x \dot{y}, A_z \dot{z}]$ ), where ( $A_x, A_y, A_z$ ) are the drag coefficient along the respective axes. Using the Newton-Euler dynamic equations in the component form the aerodynamic coefficients of drag are given by,

$$\dot{u} = (S\phi S\psi + C\Phi S\theta C\psi) \frac{T}{m} - \frac{A_x}{m} u \quad (5a)$$

$$\dot{v} = (-S\phi C\psi + C\Phi S\theta S\psi) \frac{T}{m} - \frac{A_y}{m} v \quad (5b)$$

$$\dot{w} = -g + (C\phi C\theta) \frac{T}{m} - \frac{A_z}{m} w \quad (5c)$$

The measured thrust force is co-plotted with the theoretical thrust for a near-hover condition and is in good agreement with the expected results as shown in (Fig. 9(a)). The drag coefficients are extracted using (Eqns. 5a, 5b, 5c), and the resultant drag force components are co-plotted in (Fig. 9(b)). The predominant drag force component, ( $F_{D_x}$ ), acts in the x-direction as expected. The components ( $F_{D_y}, F_{D_z}$ ) tend to zero due to the negligible  $v$  and  $w$  velocities.

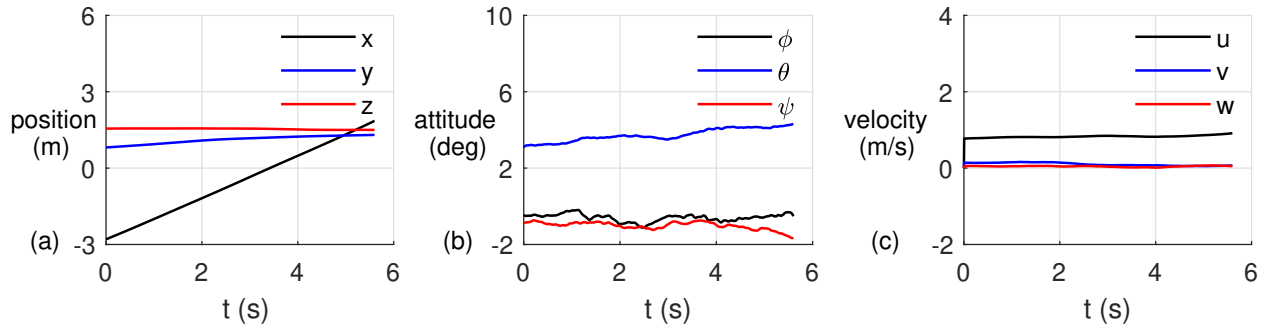


**Fig. 8 Forward level flight data for the TSRC Q7: (a) Position time history, (b) attitude time history, and (c) velocity time history.**

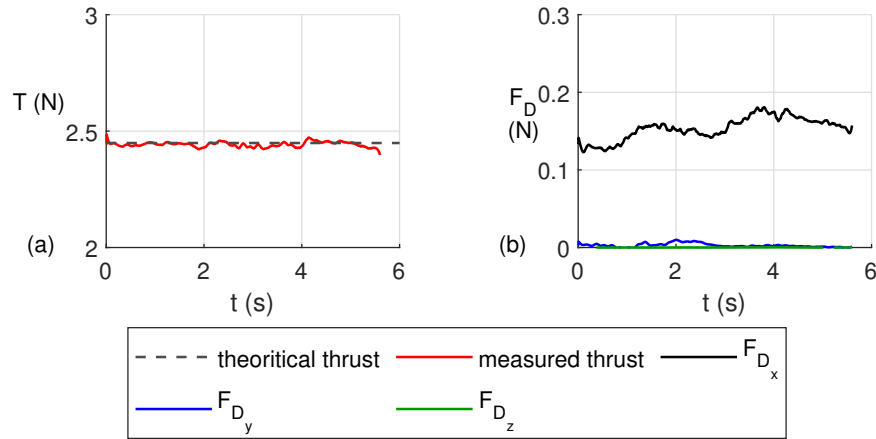


**Fig. 9 Aerodynamic forces for the TSRC Q7: (a) Measured thrust, and (b) measured drag force in the x, y, and z-directions.**

### C. Square Maneuver

The square maneuver involved flying the quad-copter in the positive x-direction, followed by a lateral translation in the negative y-direction, then the longitudinal translation in the negative x-direction, and finally another translation the positive y-direction as shown in (Fig. 10(a)). No cornering was performed and the quad-copter was maintained in a near-hover state throughout the maneuver as shown in (Fig. 10(c)).

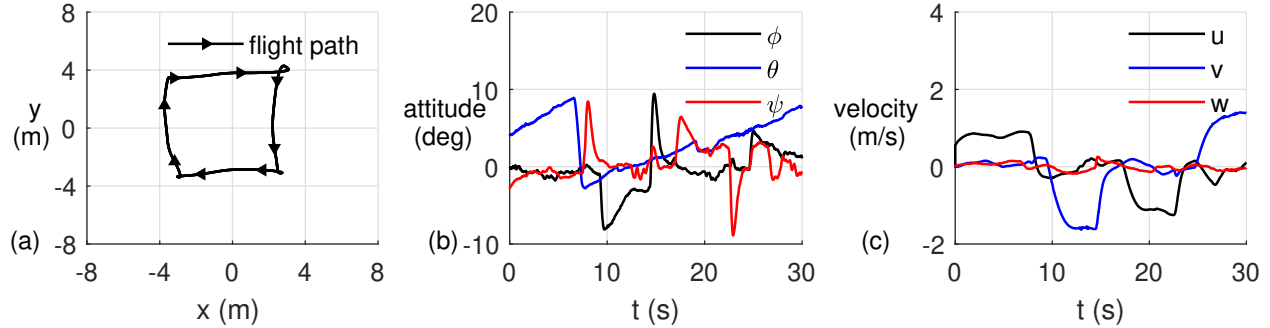


**Fig. 10 Square flight maneuver flight data for the TSRC Q7: (a) Flight path, (b) attitude time history, and (c) velocity time history.**

A multiple linear regression was performed to estimate the thrust and drag coefficients from the measured position and attitude time histories (Eqns. 3, 5a, 5b, 5c). The drag in the z-direction was assumed to be zero due to the near-hover state ( $w \approx 0$ ), and the thrust calculated from the multiple linear regression is plotted in (Fig. 11(a)), and compared the theoretical required thrust to maintain near-hover flight. Overall the trend is in agreement with the expected thrust. The magnitude of the drag force in all directions is plotted in (Fig. 11(a)). As the velocity components  $u$  and  $v$  become dominant during their respective phases of motion, the drag force primarily acts in the corresponding direction. This behavior aligns with the expectation, with minimal contribution in directions where velocity remains negligible.

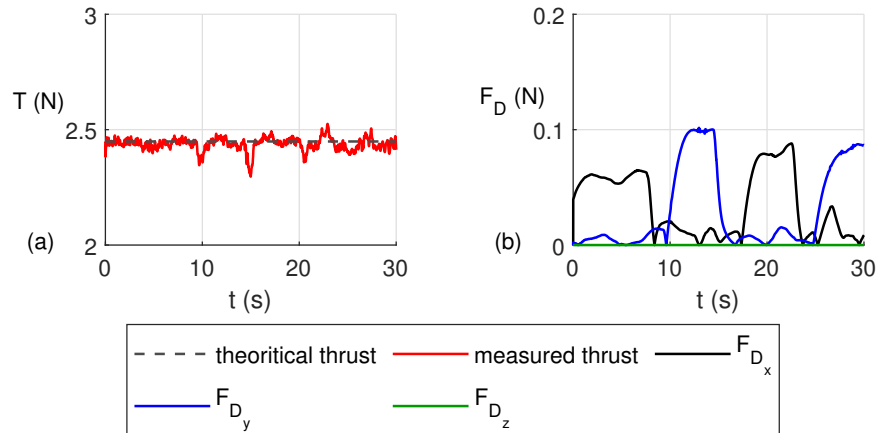


**Fig. 11 Aerodynamic forces for the TSRC Q7: (a) Measured thrust, and (b) measured drag force in the x, y, and z-directions.**

### D. Lessons Learned

Throughout this whole research project a variety of challenges have been met and worked through. Using a fully open source and build your own UAS allows any data desired to be connected depending on the accessories used with the autopilot. To add another level of validity to the experimental power and thrust data, using a hall effect sensor or exchanging the ESCs with ones would allow individual motor RPM tracking. An unexpected lesson learned was the impact of the air conditioning in the test environment creating inconsistent behaviors on the UAS during takeoff or minor deviations in results.



## E. Future Research

Taking the results from this research project and applying the lessons learned to future research could be done by modifying the flight paths, testing to find different aerodynamic data, or using the UAS for a wider range of testing outside of aerodynamics. The F450 will undergo the same testing once the stability issues are resolved and ESC data will be used to validate the thrust findings.

## V. Conclusion

From previous research, the MOCAP system at Raspet Flight Laboratory was deemed valid by testing the acceleration due to gravity and comparing it to reality. The MOCAP data was able to provide accurate translational and rotational data. Velocity and acceleration data was derived, and all the data was plotted against time, accomplishing the first goal of this research. The aerodynamics of multirotor aircraft comes with challenges that are not present with fixed wing aircraft. For example, the MOCAP collects data at a frequency of 200 Hz while the rotors spin much faster. This meant that the RPM, which is essential to thrust calculations, couldn't be tracked by MOCAP due to the aliasing effect. Two methods were used to remedy this, one being using onboard flight power data to calculate thrust while the other derived thrust using Newton-Euler equations. This data was used to establish further the validity of the system assuming thrust equals weight. On the other hand, multirotor aircraft have fewer aerodynamic forces that need to be calculated in comparison to it's fixed wing counterparts. Drag was therefore the only aerodynamic force to be investigated. Once the drag is validated, the second goal of this project will be complete. Vibrations and the stability of the aircraft directly after assembly were two factors that caused some delay in testing to ensure the data was as clean as possible. The data collected could be more precise, but the validity of the motion capture system in comparison to the autopilot.

## Acknowledgments

The authors would like to thank Mohamed El Mehdi Ouhabi, PhD. Candidate, Shreyas Narsipur, PhD., and Calvin R. Walker, and Robert R. Wolz for providing guidance with this project. A special thanks to Mississippi State University Department of Aerospace Engineering for providing the funding for the Multirotor UAS used in this project. Thank you to Mississippi State University Raspet Flight Laboratory for allowing this team to use the Autonomous Systems Research Laboratory.

## References

- [1] "Motion Capture Systems," <https://www.optitrack.com/>, 2024.
- [2] WORK, H., "F450 drone kit to build, DIY 450mm wheelbase 4-axis multi-rotor drone," [https://www.hawks-work.com/pages/f450\\_tutorial\\_video](https://www.hawks-work.com/pages/f450_tutorial_video), 2022.
- [3] ArduPilot, "Mission Planner," <https://www.mathworks.com/products/matlab.html>, 2009. Version 1.3.82.
- [4] Ouhabi M, N. S., Kim J, "Off-Board Aerodynamic Measurements of Small-UAVs in Glide and Powered Flight Using Motion Tracking," Tech. rep., Mississippi State University, Jan 2023.
- [5] WORK, H., "F450 assembly tutorial videos," <https://www.hawks-work.com/products/f450-drone-kit-to-build-diy-450mm-wheelbase-4-axis-multi-rotor-drone-kit-b>, 2024.
- [6] Mohamed El Mehdi Ouhabi, S. N., "Off-Board Characterization of sUAV Aerodynamics and Stability Derivatives Using Motion Tracking," AIAA paper 2024-3761, 2024.
- [7] Natural Point, "Motive," <https://optitrack.com/software/motive/>, 1996. Version 3.1.4.
- [8] MathWorks, "MATLAB," <https://www.mathworks.com/products/matlab.html>, 2022. Version 2022b.
- [9] Mohamed El Mehdi Ouhabi, J. K., Shreyas Narsipur, "Off-Board Aerodynamic Measurements of Small-UAVs in Glide and Powered Flight Using Motion Tracking," AIAA paper 2023-0813, 2023.
- [10] Ouhabi, M. E. M., and Narsipur, S., "Off-Board Aerodynamic Measurements of Small-UAVs in Glide Flight Using Motion Tracking," *The Aeronautical Journal*, 2025. <https://doi.org/10.1017/aer.2024.131>.
- [11] Sanca A, A. P., Cerqueira J, "Dynamic Modelling of a Quadrotor Aerial Vehicle with Nonlinear Inputs," 2008. <https://doi.org/10.1109/LARS.2008.17>.